SCIENTIFIC PAPERS
OF THE UNIVERSITY OF PARDUBICE
Series A
Faculty of Chemical Technology
4 (1998)

FACTORS AFFECTING CROSS-FLOW MICROFILTRATION OF DISPERSIONS

Petr MIKULÁŠEK
Department of Chemical Engineering, University of Pardubice,
CZ-532 10 Pardubice

Received February 19, 1997

This paper deals with the use of microfiltration in fouling dispersion systems and discusses the means available to the process designer to minimize the effects of fouling and take them into account when performing the design. The results of recent work which show how the characteristic parameters of membrane (pure water flux and pore size distribution), the effects of operating parameters (composition of dispersion, cross-flow velocity, transmembrane pressure), and the feed flow management (hydrodynamic) methods to improving the flux (the cross-flow system in the presence of a fluidized bed and the rotating membrane system) can contribute to the minimisation of fouling and process optimalization.

Introduction

Cross-flow membrane microfiltration is a separation process for removal of dispersed matter with particles ranging from 0.05 to 10 μm from a liquid stream by forcing the liquid to pass through a porous membrane. As opposed to dead-end microfiltration, where the dispersion is forced normal to the membrane, the

dispersion in cross-flow filtration is forced tangential to the membrane surface. This generates a number of forces which tend to remove the deposited layers from the membrane surface thus helping to keep the membrane relatively clean. The main applications of this process are in the production of ultrapure water, the processing of food and dairy products, the recovery of electrodeposition paints, the treatment of oil and latex emulsions and in biotechnology-oriented applications such as fractionation of fermentation broths and high performance reactors for enzymatic and fermentation processes.

However, the present cross-flow membrane processes for liquid feed streams are still complicated by the phenomena of membrane fouling and of concentration polarisation in the liquid boundary layer adjacent to the membrane wall. Concentration polarisation and membrane fouling are major concerns in the successful use of a membrane-based separation operation, as their net effect is to reduce the permeate flux, thereby resulting in loss of productivity. Therefore, there is a tremendous potential to reduce or control concentration polarisation and fouling in membrane processes and hence alleviate these limitations. The flux decline due to membrane fouling is frequently masked by changes in membrane properties, or the feed solution, or the development of concentration polarisation. The concentration polarisation results in a localised increase in the solute concentration on or near the membrane surface. This solute build-up lowers the flux due to an increase in hydrodynamic resistance in the mass boundary layer and due to an increase in local osmotic pressure resulting in a decreased net driving force. However, concentration polarisation effects are reversible, since they can be reduced by decreasing the trans-membrane pressure or lowering the feed concentration. Fouling effects, on the other hand, are usually characterised by an irreversible decline in the flux. Although both concentration polarisation and membrane fouling cannot generally be avoided in membrane separations there are several possible approaches to reducing or controlling their extent. A morphological analysis of ways reducing concentration polarisation and fouling is presented for example in literature [1,2].

The degree to which process design can affect the degree of fouling thus includes the characterisation and choice of membrane, operating parameters, and flux enhancement methods. This paper will briefly review these processes in turn indicating some of the design solutions which have been taken.

Ceramic membranes can be characterised in terms of pore size, pore size distribution, interfacial area, void fraction, surface charge, tortuosity, etc. An important aspect of chemical engineering calculations for flow through a porous medium is the prediction of the fluid pressure drop, and determination of its dependence on the flow properties of the fluid and on the geometry of the medium. The characterisation of the available pores is very important to manufacturers of membrane filters giving an accurate representation of the condition of the filter. The pure water flux is a measure of the hydraulic permeability of the membrane, and is

the most common parameter used in microfiltration. Although steady-state flux during membrane filtration is the main process feature, the pure water flux is not an independent membrane characteristic. It is a result of the interplay of pore size (distribution), tortuosity and thickness of the active layer of the membrane [3].

Alumina microfiltration membranes were tested for use as part of a microfiltration unit for the treatment of latex dispersions. In this operation tubular microfiltration membranes were used with the mean pore diameter equal to 0.1 μm. The results of this study indicated that the characteristic parameters of the membrane (determined by the liquid displacement method) are relevant for predicting the transport properties of alumina microfiltration membranes. A limiting flux was observed which depended on the polymer nature, pressure difference, feed velocity, and particle to membrane pore diameter ratio. The decrease in the flux of permeate was attributed to the resistance of the cake (gel) layer formed on the membrane or blocking of the pores in the membrane. By these means, low permeate fluxes were obtained at relatively high solution velocity.

Many different approaches can be taken to improve the flux in these systems. The basic methods involve: changes in surface characteristics of the membrane, pretreatment of the feed, and fluid management methods [1]. The feed flow management (hydrodynamic) approach to improving the flux is either to reduce the concentration polarisation by increasing the mass transfer away from the membrane or to reduce fouling based on increasing the wall shear rate and/or scouring the membrane surface. Therefore, the last part of this paper shows the effects of these factors on the performance of the cross-flow microfiltration system in the presence of a fluidized bed and the rotating membrane system. The irregular flow of the feed around both the membrane surface and fluidized bed particles as well as the movement of the particles themselves can be responsible for the improved permeate flux. A rotating module design represents another approach of minimising the flux decline problems. Here we present the experimental results carried out in the device containing concentric cylinders of which the inner is a rotated tubular ceramic membrane causing shear stresses in the feed flow, centrifugal force away from the membrane, and flow instabilities in the annulus.

Experimental

Membranes

The ceramic membrane used for testing was an alumina-based, tubular, internal-pressure-type membrane (manufactured by TERRONIC in the Czech Republic). It had an inner diameter of 6 mm, outer diameter 10 mm, and was produced either as a thick α-alumina layer (mono-layered) or a thin α-alumina layer on the top of the support (multi-layered). For this type of asymmetric membrane, the slip-casting

method was used. In our characterisation studies, several membranes were used with a nominal pore diameter from 0.1 to 1.5 μm. The void volume of the mono-layered membrane samples was determined by liquid flooding and by measuring the membrane thickness. The ceramic membranes used for cross-flow microfiltration were configured as single cylindrical tubes 0.1 m and 0.2 m long, 6 mm ID and 10 mm OD with the mean pore diameter equal to 0.1 μm. However, the ceramic membranes used for rotating and fluidized bed system were configured as single tubes of 12 mm ID and 17 mm OD consisting of a thin α-alumina layer on the top of a support.

Feeds

Seven different feeds were used in this study. These varied from deionized water, through aqueous dispersions of powdered material to the surfactant stabilised latex dispersions (poly(vinyl acetate) with different composition, Duvilax LM-52, BD-20, latex paint V 2011, and acrylic copolymer Sokrat 6492). Concentration of dispersed matter varied from 1 % to 3% (w/w). In the fluidized bed experiments model dispersions were created either by aqueous suspensions of microsized alumina powder or submicron latex particles. The latter were also used in rotational experiments. The sizes of dispersed particles were determined using a particle sizer BI-90 (Brookhaven Instruments Corp.) and SediGraph 5100 (Micromeritics), respectively.

Equipment

The flow of water through á-alumina microfiltration membranes (length 20 mm) at various pressure was investigated using the apparatus shown in Ref. [4]. The permeate mass and the filtration pressure data were synchronised by use of a pressure transducer interfaced with a computer. Therefore, simultaneous measurements of the cumulative permeate mass and the pressure were obtained. These measurements covered a range of constant filtration pressures (ΔP) from 100 to 300 kPa.

A description of the porometer for determination of the pore size distribution is given in Refs [5,6]. The porometer uses a common liquid displacement technique that is adapted from the ASTM F316-80 procedure [7], and determines pore size distribution from 0.05 μm to 10 μm. It uses either an air or nitrogen external pressure source of up to 1 MPa. It consists of a flowmeter, special sample holder, and 0 – 1 MPa pressure sensor in conjunction with an XY plotter.

The ceramic filter (length 35 mm) is inserted into the sample holder such that the ends of the sample are sealed. The sample holder is closed hand-tight, and is

subjected to increasing pressure and flow of dry air or nitrogen. The ceramic filter is then filled with a wetting liquid having low surface tension, and is again subjected to increasing pressure and flow of nitrogen. Liquid is expelled from the pores when the pressure overcomes the capillary attraction of the liquid in the pores. Monitoring the initial flow of gas, i.e. the point at which gas is first seen to pass through the sample (the bubble-point) allows calculation of the maximum pore size. From these two tests (dry and wet curves), pore distributions can be calculated [5]. The method allows the same specimen to be used for both dry and wet runs, thus eliminating the sampling problem associated with using different specimens in two separate holders.

The cross-flow filtration unit was the same as in Refs [8,9], but in this case, the dispersions were circulated through the module by a diaphragm pump with a damper from the base of the retentate container under pressure into the membrane filter, while both the concentrated dispersion and the permeate were recirculated back into the retentate container. Therefore, the concentration in the container remained virtually constant. The unit allowed studies in which the transmembrane pressure and the cross-flow velocity were independently varied.

The fluidized bed filtration system consisted mainly of a microfiltration module, a centrifugal pump, a storage tank equipped with a thermal regulation system, and a temperature and pressure control system. Fluidized particles were either glass beads of 1.47 mm diameter and 2506 kg m^{-3} density or stainless steel beads of 1.00 mm diameter and 7506 kg m^{-3} density. For each experiment with fluidized bed, the column was filled with solids in such a way that the total expanded bed height was equal to membrane length. The corresponding solid loading and superficial velocities were known from preliminary results on hydrodynamics obtained in a transparent tube with the same diameter as the membrane.

The rotating filtration system consisted of an outer, transparent, acrylic-glass cylinder, an inner rotating cylinder, and a flange. The inner cylinder was formed by an alumina ceramic membrane with a length of 0.1 m, an effective area of 50 cm^2 and outer skin layer with the mean pore diameter 0.1 μm. The feed was pumped into the annular gap formed by two cylinders with a peristaltic pump. The mean transmembrane pressure in the annular gap was monitored by regulating a simple valve which creates a backpressure along the membrane to the outlet of the pump. The pressure was measured at the wall of the outer cylinder of the filtration unit.

Results and Discussion

Characterisation of Membranes [4,5,6]

Pure Water Flux

An important parameter when determining membrane rejection characteristics is the mean pore diameter of microfiltration membranes having a narrow pore-size distribution. In general, the smaller the pore diameter, the higher will be the rejection coefficient of particulates/solutes of a greater nominal size. However as the pore size decreases, the permeability to liquid also rapidly decreases. Typical pure water (prefiltered deionized water) fluxes as a function of the pressure difference are shown in Fig. 1 for different microfiltration alumina membranes.

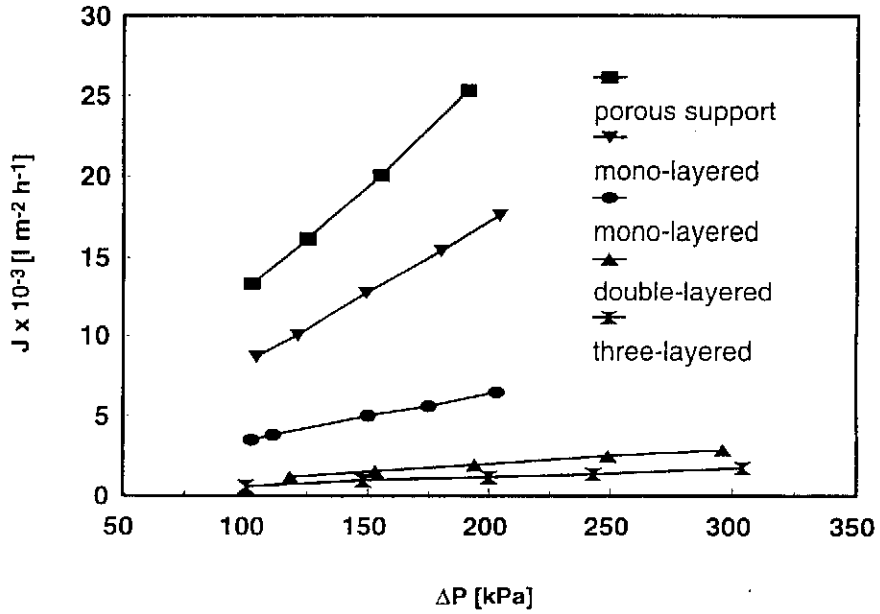

Fig. 1 Flux of water through various types of alumina membranes

As previously mentioned [4], the function of the support is to give strength to the system. Its permeability should not significantly lower the total permeability. For a multi-layered alumina membrane, the permeability should be determined mainly by the permeability of the active layer. The permeability of the active layer can be calculated by assuming a series-resistance (approximately inversely proportional to permeability) model for the multi-layer system. The strength of a porous material usually decreases with increasing permeability, and the information

obtained from those measurements can be used to choose an optimum active layer/support combination for a particular application.

Pore Size Distribution

These results are presented as a plot of percentage pore area distribution versus pore diameter, including a table of minimum, mean and maximum pore sizes. Figure 2 shows the distribution curves for a porous support, mono-layered, and multi-layered Terronic ceramic membranes [4]. The pore-size distribution measurements clearly emphasise the influence of the preparation conditions. The data presented in Fig. 2 also indicate that the multi-layered ceramic membranes used in these studies have a very narrow pore-size distribution. This narrow distribution is extremely useful for accurately predicting the performance of tubular ceramic membranes in different applications.

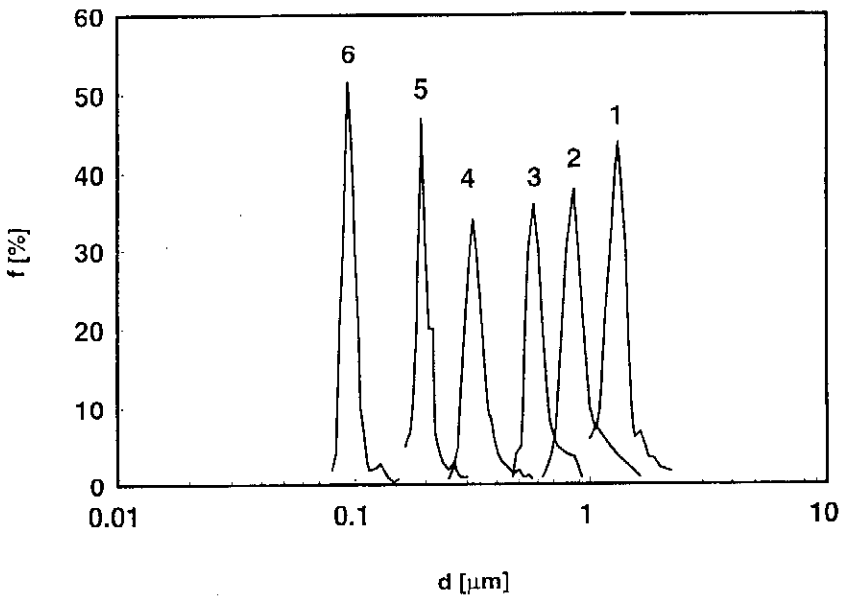

Fig. 2 Pore area distribution versus pore diameter for the Terronic alumina membranes: (1) porous support; (2), (3), (4) mono-layered; (5) double-layered; (6) three-layered

Influence of Dispersion Composition on Permeate Flux

The flux during microfiltration of dispersions was substantially lower than the pure water flux—ranging from 1 – 30% of clean water flux, which indicates cake (gel) or pore blocking control in all the experiments.

In the majority of cases the experimental data showed a trend with higher fluxes for the acrylic copolymer dispersion compared with the poly(vinyl acetate) dispersions (see Fig. 3). The lowest flux occurred with poly(vinyl acetate) dispersion Duvilax LM-52 which is manufactured with a protective colloid (poly(vinyl alcohol)) and contains the polymer, initiator, buffer and perhaps a molecular weight regulator. Therefore, this dispersion has a poor mechanical stability during microfiltration because the protective colloid may be stripped from the surface of the polymer particles when the dispersion becomes diluted. The higher steady-state flux was observed for poly(vinyl acetate) paint V-2011 containing pigments, filling agents and some surfactants. In this case the latex paint stability can be improved by the presence of physically adsorbed non-ionic polymer chains on the surface of the particles by complete interaction between the particular dispersion-surfactant combination and by the contents of pigments and filling agents.

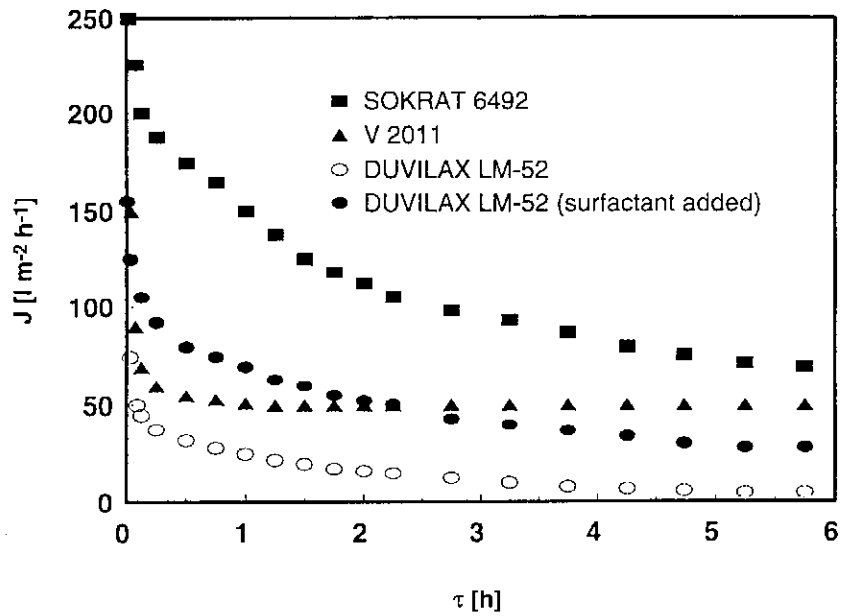

Fig. 3 Permeate flux versus time for dispersion microfiltration (concentration, 1% w/w; ΔP = 100 kPa)

Effect of Surfactant on Flux

Surfactant addition is usually the most effective way to enhancing dispersion stability as a pretreatment prior to microfiltration. Experience has shown that the surface tension of the dispersions may be indicative of their stabilities under microfiltration process conditions. However, it should be noted that low surface tension does not guarantee a favourable dispersion stability for microfiltration. Rather, the stability depends on the complete interaction between the particular dispersion-surfactant combination. About 5% (wt. surfactant/wt. dispersion) of an anionic surfactant (Disponil AES 60, Henkel, Germany) was added to the diluted Duvilax LM-52 to stabilise it against mechanical degradation. As illustrated in Fig. 3, nearly four times higher flux was obtained for the surfactant-stabilised dilute dispersion. It seems that steric dispersion stabilisation alone yields dispersion in the gel layer unstable and agglomerated into an impervious film. However, mixed steric-electrical stabilisation inhibits particle double-layer compression and consequently compaction of the foulant layer which is formed on the membrane surface.

Effect of Transmembrane Pressure Difference on Flux

In Fig. 4 the steady-state flux data are plotted versus the transmembrane pressure difference for acrylic copolymer and PVC dispersions. If the particles were bigger than the pores, i.e., in the system with PVC dispersion, it was found that the flux increases linearly with pressure difference at low values up to a critical pressure difference, then the rate of increase decreases, and finally the flux becomes nearly independent of pressure difference at high values. These findings support the well-known fact that both the membrane and the cake resistance are dominant for low pressure differences, whereas the boundary layer resistance is dominant for high pressure differences.

The pressure dependence of steady-state flux of acrylic copolymer dispersions is also shown in Fig. 4. In comparison with the PVC dispersion results, there is an optimum pressure below which the driving force is too low and above which increased fouling causes a large reduction in flux. This could be attributed to the formation of a filtration cake with higher resistance once the deposited particles undergo compaction under higher transmembrane pressures. Thus a more likely hypothesis is that the initial internal membrane fouling is both feed velocity and pressure dependent, and its degree is affected by the membrane pore size. We conclude that both the internal fouled membrane and secondary membrane are the dominant resistance.

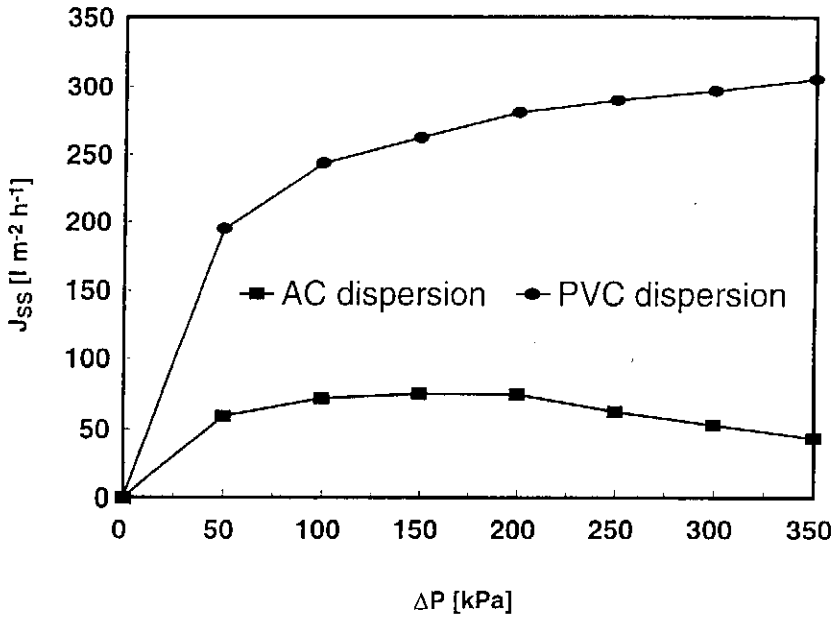

Fig. 4 Variation of the flux with transmembrane pressure difference for 0.95 m s^{-1} feed velocity

Effect of Cross-Flow Velocity on Flux

Values of flux vs. time for various mean velocities are plotted in Fig. 5 for PVC/water dispersion. As the filtration process continues, the filtration rate decreased gradually, and as a result the drag on the solutes which constitute the cake decreases. Consequently, the cake begins to be swept away, and then the filtration rate tends to approach a plateau or dynamically balanced value. The thickness of the cake layer and its hydraulic resistance decreases with increasing cross-flow velocity (i.e., compare steady-state flux for feed velocity 0.94 and 3.00 m s^{-1}).

Comparison with Theoretical Predictions

Assuming boundary layer control in the cross-flow microfiltration of the dispersions used, the estimates of steady-state flux were calculated from the film theory using both Stokes–Einstein diffusion [11] and shear-induced diffusion [12]. For particles of the size range studied, nondiffusive transport can also be dominant. Thus the theoretical predictions given by the model of lateral migration [13] were determined.

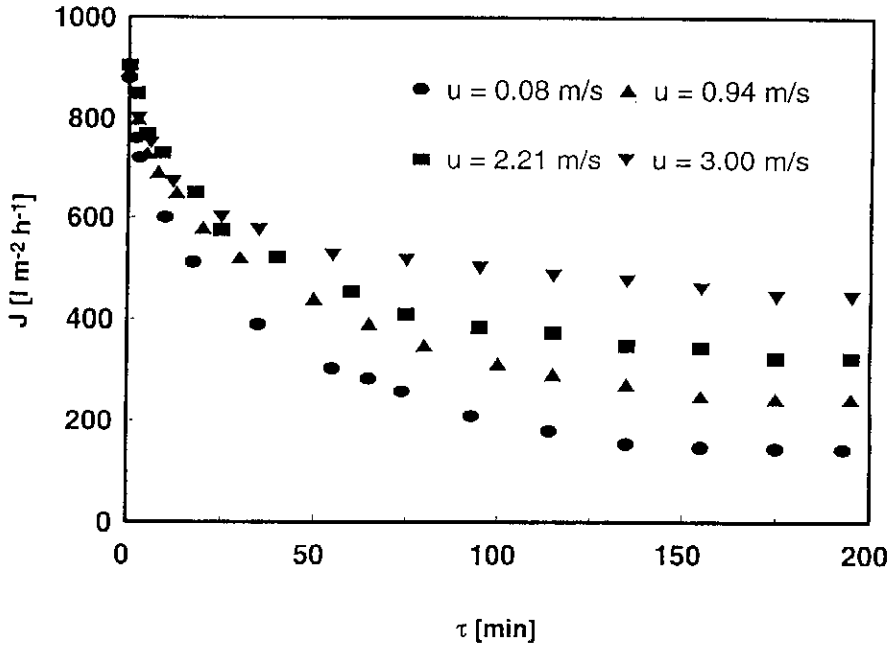

Fig. 5 Permeate flux versus time for microfiltration of PVC/water dispersion (concentration, 1% w/w; ΔP = 100 kPa)

In contrast to the polydisperse systems used in our experiments, the theoretical models were derived for idealised dispersions of equisized spheres. Therefore the models were examined with particular attention being paid to particle size effects.

The decrease in flux with increasing particle diameter is predicted using Stokes-Einstein diffusion, whereas increasing flux is obtained for shear-induced diffusivity and lateral migration. The transition from ultrafiltration-type behaviour (steady-state flux vs. decreasing particle diameter) to microfiltration-type behaviour (steady-state flux vs. increasing particle diameter) should occur at a particle diameter of about 0.35 μm for the system with acrylic copolymer dispersion. This value is outside the size distribution of the dispersion studied (see Ref. [10]). Therefore, according to the models used, the Stokes-Einstein diffusion should prevail. If we assume that the behaviour is dominated by the smallest particles, present in the feed, the agreement of the experimental steady-state flux with predictions is apparently satisfactory. In contrast to the Stokes-Einstein diffusion model, the shear-induced diffusion model gives several times lower values for the steady-state flux. The inertial lift theory in this case underpredicts the steady-state fluxes by three orders of magnitude.

The system with PVC dispersion was chosen as an alternative to the acrylic copolymer dispersion, where the larger particles had a higher steady-state permeate

flux (310 $l\,m^{-2}\,h^{-1}$). The low values of the relative system resistance (the ratio of the cake and membrane resistance) indicate that both the cake and membrane resistances were important in most of the experiments. Also, it has been shown that the boundary layer resistance is dominant for high pressure differences. The dependence of the limiting steady-state flux versus particle diameter is shown in Fig. 6. When it is compared to results for the acrylic copolymer dispersion, two features are noteworthy. First, the Stokes–Einstein diffusion-based model underpredicts the limiting steady-state flux by several orders of magnitude. In contrast, the shear-induced diffusion and lateral migration models gave prediction of the right order of magnitude. Second, the predicted limiting steady-state flux is strongly particle diameter dependent. This phenomenon is not as pronounced in the case of the lateral migration model. Nevertheless, it seems that the polydisperse microfiltration feed used cannot be easily characterised by a simple average particle diameter for the purpose of these model calculations.

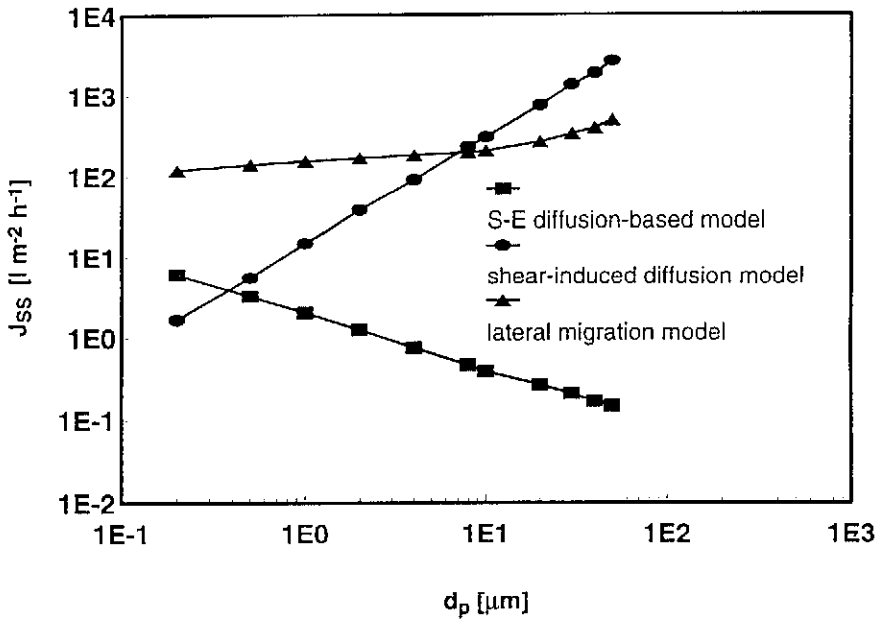

Fig. 6 Predicted variation of the flux with particle diameter for microfiltration of PVC/water dispersion at 0.94 m s^{-1} feed velocity (Re = 5640; γ = 1254 s^{-1})

Fluidized Bed Microfiltration [14,15]

The values of permeate fluxes versus time show, in the course of microfiltration in the presence of fluidized particles, the same shape of $J(\tau)$ curves compared to those of the empty tube experiments. However, a strong and non-monotonous dependence of permeate flux at steady-state, J_{SS}, upon the superficial fluid velocity and/or porosity may be observed. As a rule, the values of the steady-state permeate flux in the fluidized bed system are superior to the ones obtained, when no fluidized medium was used (in an empty tube), with a maximum ratio of 1.5 (Fig. 7). On the whole, these results agree well with scattered information on the intensification of microfiltration by a fluidized bed already published in literature [16]. Fluidized particles act as obstacles to the fluid flow in the same way as if they were fixed within a membrane; because of their presence, turbulence is increased and concentration polarisation is weaker and/or cake layers are considerably thinner than in the empty tube. However, particle motion may be thought of as being responsible for strong and continuous erosion of particle deposits at the wall. Particle-cake contacts are certainly more effective than turbulence when ε is around 0.8, when slugging of a fluidized bed was observed in the course of preliminary experiments on hydrodynamics obtained in a transparent tube.

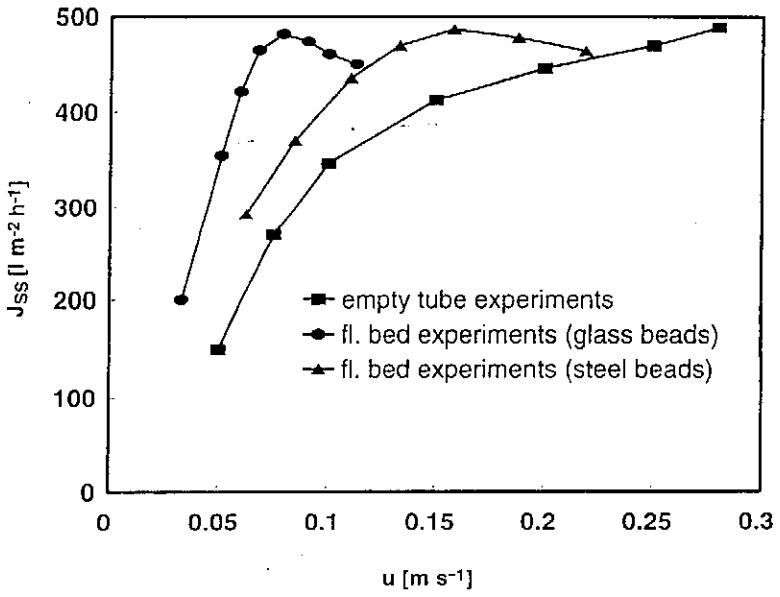

Fig. 7 Variation of steady-state permeate fluxes with superficial velocity for alumina powder dispersion microfiltration (ΔP = 50 kPa)

A more extensive study of the effect of a shear rate on flux was made in studies comparing the steady-state flux of empty tube and fluidized bed systems. The results show that an operational run time of approximately 1 h produces a reasonable flux where it may be assumed that the plateau corresponding to the steady-state values was reached. To facilitate comparison between the two different systems considered, the shear rate at the inner membrane surface, assuming Newtonian fluid behaviour of the alumina dispersion and fully-developed laminar flow, was approximated for the cross-flow tube system by Eq. (1)

$$\gamma = \frac{8u}{D} \tag{1}$$

and for fluidized bed system by the relationship [17]

$$\gamma = \frac{12u(1-\varepsilon)}{\varepsilon^2 d_p} \tag{2}$$

substituting the corresponding experimental values of superficial velocity u and bed porosity ε, respectively.

As shown in Fig. 8, the steady-state permeate flux in the fluidized bed system was non-monotonous with the estimated shear rate at the membrane inner wall. It is evident that the flux had not reached its maximum at the lower shear rate, and bed porosity ($\varepsilon = 0.9$), respectively. On the contrary, the flux in the empty tube system was nearly linear with increasing shear rate above the value of approximately 30 s^{-1} at the membrane surface. It follows from Fig. 8 that the steady-state permeate flux in empty tube and fluidized bed systems was approximately the same for the value of the shear rate close to 180 s^{-1}. On the other hand, this value of the steady-state permeate flux (approximately 480 $l\,m^{-2}\,h^{-1}$) was obtained in the empty tube system using the superficial velocity 3.5 times higher than that observed in the fluidized bed system.

Rotational Microfiltration [18,19,20]

The influence of transmembrane pressure and angular velocity on the flux was studied with dilute latex dispersions in a recycle mode. Figure 9 shows the results of these experiments. As generally is the case in cross-flow micro-filtration, asymptotic curves of flux versus pressure are obtained with different levels depending on the angular velocity. On the basis of Fig. 9 we speculate that the resistance to flow through the gel-cake layer is dependent on transmembrane pressure (through compressibility, for example) and inversely dependent on angular velocity (through a balance between convective drag to the membrane and inertial lift, shear-induced diffusion, and centrifugal force away from the membrane).

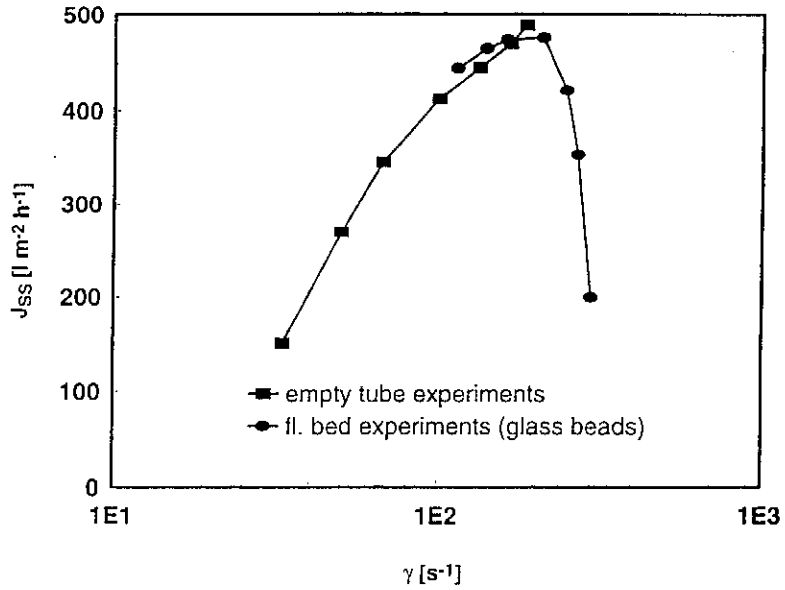

Fig. 8 Variation of steady-state permeate flux with wall shear rate for alumina powder dispersion microfiltration (ΔP = 50 kPa)

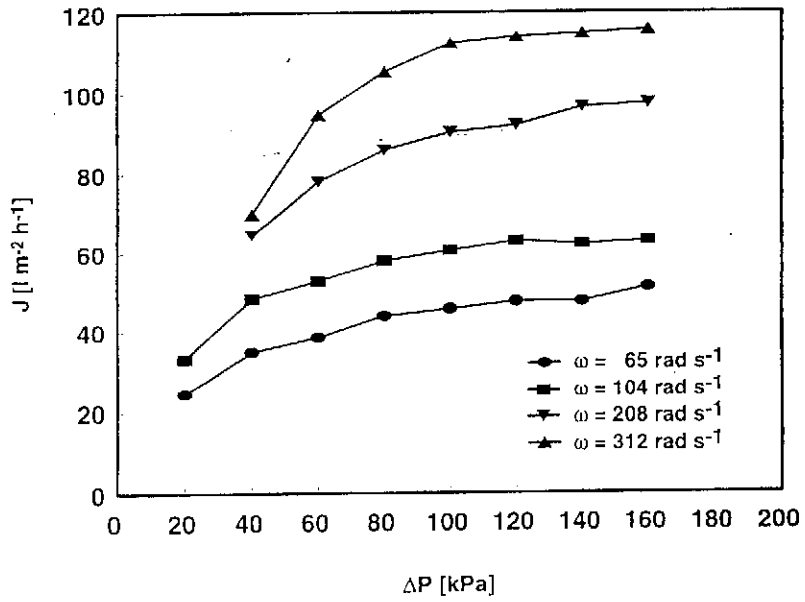

Fig. 9 Permeate flux versus actual transmembrane pressure for latex dispersion rotational microfiltration at different angular velocity (concentration, 1% w/w)

The dominant influence of the angular velocity was studied by separate experiments under constant-pressure conditions. In all cases a substantial decrease of cake resistance with increasing angular velocity is observed. This cannot be achieved simply with a stationary membrane in the cross-flow microfiltration system because a shear rate increase due to increasing the flow leads to a rise in pressure drop and therefore a decrease of transmembrane pressure.

The study of the effect of a shear rate on flux was made in studies comparing the steady-state flux of tangential cross-flow and rotary systems. The shear rate at the membrane surface for azimuthal flow in an annulus with a porous wall on the rotating inner cylinder was solved for the narrow-gap approximation in accordance to results mentioned in Ref. [20].

As shown in Fig. 10, the steady-state flux in the rotary system was approximately linear with the shear rate at the membrane surface; the flux had not reached a maximum at $\omega = 365$ rad s^{-1}, the maximum angular velocity of the prototype. These results can be realised by assuming that deposited particles remain on the membrane when a friction force proportional to the transmembrane pressure exceeds the drag from the shear rate. In contrast, the flux in the cross-flow system was nearly constant with increasing superficial velocity above a shear rate of approximately 3000 s^{-1} at the membrane surface.

It follows from Fig. 10 that at conditions yielding identical shear rates, the membrane flux in the rotary system is approximately twice that observed in the tangential cross-flow system. A three- to four-fold higher shear rate was required in the cross-flow system to achieve the same permeate flux as in the rotary system.

Conclusion

Microfiltration alumina membranes with different properties were used to characterise their behaviour. The effect of the support tube resistance on the permeability of the multi-layered alumina membranes was determined. These results can be used to select the optimum active layer/support combination.

Tubular ceramic membranes could be satisfactorily characterised using the porometer and non-destructive low-pressure liquid-displacement technique. The designed system allows fast, precise, and reproducible determination of the parameters characterising the active pore size of ceramic membranes. The narrow pore-size distribution of these ceramic membranes has provided some understanding of the behaviour in terms of the flux and rejection of different process streams.

The influence of dispersion composition and the effects of operating parameters such as cross-flow velocity, transmembrane pressure difference, and addition of surfactant on flux were studied. The experimental data presented have shown that filtration flux during cross-flow microfiltration of dilute dispersions is very much dependent on the species of the dispersions and on flow velocity. The

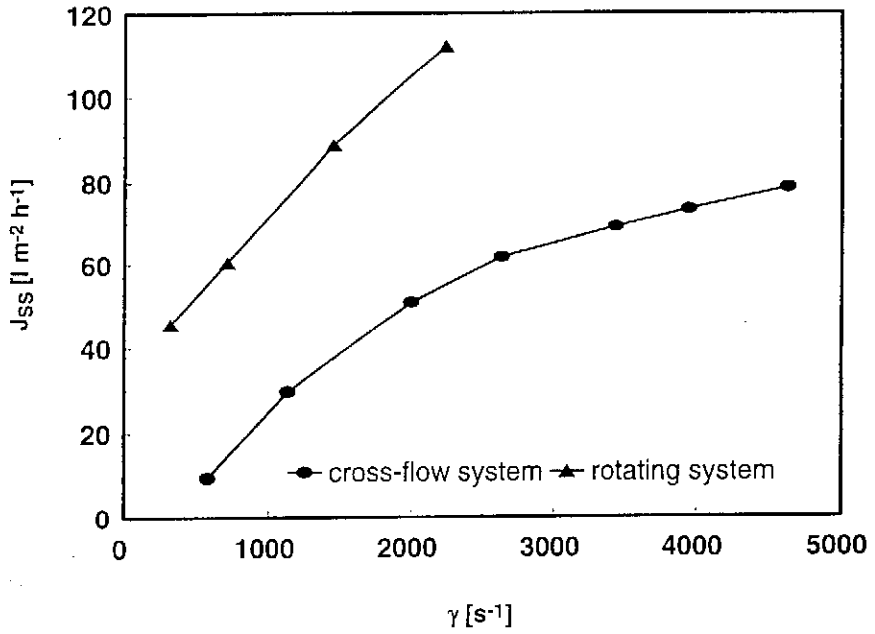

Fig. 10 Steady-state permeate flux as function of shear rate for the cross-flow system and the rotating system (concentration, 1% w/w)

changes in filtration rate may not be explained simply in terms of particle size distribution or according to the conventional descriptions of Brownian diffusion, inertial lift, or shear-induced back diffusion; therefore, polydisperse systems studied here are too complex at present to allow for the quantitative description of such a phenomenon.

The use of turbulence-promoting fluidized particles resulted in a significant increase of permeate flux through the membrane. In this case, the improved permeate flux that is achieved is due to the combined action of turbulence and particle motion (collision of particles with membrane wall). This reduces the thickness of the surface boundary layer and also reduces the hydraulic resistance of concentration polarisation and/or cake layers. However, it has been noticed that the flux reaches a maximum for the optimum bed porosity, dependent on the superficial velocity of the feed.

The superior hydrodynamics of rotary membrane filtration result in permeate fluxes several times higher than those for a tangential cross-flow microfiltration system with a tubular membrane. The wall flux of latex dispersions through a microfiltration membrane increased as the angular velocity (i.e., the rotational speed) of the filter was increased. Both the shear rate and centrifugal force on a sphere in the annular gap of the filter enhanced the reduction of membrane fouling.

In general, it is shown that by carefully analysing such operating parameters as the permeability and pore size distribution of membrane, composition of a dispersion, cross-flow velocity, transmembrane pressure difference, and the feed flow management methods, it may be possible to determine the various transport and fouling types of behaviour which are extremely valuable for process optimization.

Symbols

d	diameter of the pore, m
d_p	diameter of fluidized particles, m
D	inner diameter of the membrane tube, m
J	permeate flux, $l\,m^{-2}\,h^{-1}$
J_{SS}	steady-state permeate flux, $l\,m^{-2}\,h^{-1}$
ΔP	transmembrane pressure, Pa
τ	time, s
u	superficial velocity, $m\,s^{-1}$
γ	shear rate, s^{-1}
ε	bed porosity

References

1. Mikulášek P.: Collect. Czech. Chem. Commun. **59**, 737 (1994).
2. Belfort G., Davis R.H., Zydney A.L.: J. Membr. Sci. **96**, 1 (1994).
3. Bhave R.R. (ed.), *Inorganic Membranes, Synthesis, Characteristics and Applications*, Van Nostrand Reinhold, New York 1991.
4. Mikulášek P., Doleček P., Šedá H., Cakl J.: Dev. Chem. Eng. Mineral Process. **2**, 115 (1994).
5. Mikulášek P., Doleček P.: Sep. Sci. Technol. **29**, 1183 (1994).
6. Mikulášek P., Doleček P., Rambousek V., Cakl J., Šedá H.: Ceramics-Silikáty **38**, 99 (1994).
7. ASTM Standard Test Method no. F316-80, *The American Society for Testing and Materials*, p. 303–309 Philadelphia 1980.
8. Mikulášek P.: Recents Prog. Genie Procedes **6**(22), 305 (1992).
9. Mikulášek P., Cakl J.: Desalination **95**, 211 (1994).
10. Cakl J., Mikulášek P.: Sep. Sci. Technol. **30**, 3663 (1995).
11. Davis R.H., *Membrane Handbook* (W.S. Ho, K.K Sirkar, eds), p. 483, Van Nostrand Reinhold, New York 1991.
12. Zydney A.L., Colton C.K.: Chem. Eng. Commun. **47**, 1 (1986).
13. Drew D.A., Schonberg J.A., Belfort G.: Chem. Eng. Sci. **46**, 3219 (1991).

14. Mikulášek P.: Collect. Czech. Chem. Commun. **60**, 2074 (1995).
15. Mikulášek P., Filandrová L.: Dev. Chem. Eng. Mineral Process. **3**, 139 (1995).
16. Rios G.M., Rakotoarisoa H., Tarodo de la Fuente B.: J. Membr. Sci. **34**, 331 (1987).
17. Machač I., Mikulášek P., Ulbrichová I.: Chem. Eng. Sci. **48**, 2109 (1993).
18. Mikulášek P., Pimbley J.M., Belfort G.: *Symposium on Engineering of Membrane Processes*, Garmisch-Partenkirchen 1992.
19. Belfort G., Mikulášek P., Pimbley J.M., Chung K.Y.: J. Membr. Sci. **77**, 23 (1993).
20. Mikulášek P., Doleček P.: Sep. Sci.Technol. **29**, 1943 (1994).